

# DEVELOPMENT OF A SPECTROMETER FOR PROTON DRIVEN PLASMA WAKEFIELD ACCELERATED ELECTRONS AT AWAKE

L. Deacon, S. Jolly, F. Keeble, M. Wing\*, UCL, London, United Kingdom  
 B. Biskup†, E. Bravin, A. Petrenko, CERN, Geneva, Switzerland

## Abstract

The AWAKE experiment is to be constructed at the CERN Neutrinos to Gran Sasso facility (CNGS). This will be the first experiment to demonstrate proton-driven plasma wakefield acceleration. The 400 GeV proton beam from the CERN SPS will excite a wakefield in a plasma cell several meters in length. To observe the plasma wakefield, electrons of 10–20 MeV will be injected into the wakefield following the head of the proton beam. Simulations indicate that electrons will be accelerated to GeV energies by the plasma wakefield. The AWAKE spectrometer is intended to measure both the peak energy and energy spread of these accelerated electrons. Improvements to the baseline design are presented, with an alternative dipole magnet and quadrupole focussing, with the resulting energy resolution calculated for various scenarios. The signal to background ratio due to the interaction of the SPS protons with upstream beam line components is calculated, and CCD camera location, shielding and light transport are considered.

## INTRODUCTION

Proton bunches are the most promising drivers of wakefields to accelerate electrons to the TeV energy scale in a single stage. An experimental program at CERN — the AWAKE experiment [1, 2] — has been launched to study in detail the important physical processes and to demonstrate proton-driven plasma wakefield acceleration.

AWAKE will be the first proton-driven plasma wakefield experiment world-wide and will be installed in the CERN Neutrinos to Gran Sasso facility [3]. An electron witness beam will be injected into the plasma to observe the effects of the proton-driven plasma wakefield: plasma simulations indicate electrons will be accelerated to GeV energies [4]. In order to measure the energy spectrum of the witness electrons, a magnetic spectrometer will be installed downstream of the exit of the plasma cell. The design of the spectrometer was outlined in [5]. This paper will present the updated spectrometer design along with estimated energy resolution for various quadrupole and magnet settings.

## SPECTROMETER DESIGN

### Dipole Magnet

As a change to the previous design [6], a smaller, lighter and more efficient C-shaped magnet (HB4) was considered as an alternative to the window-shaped dipole (MBPS). The energy measurement uncertainties were also compared (see

\* and DESY, Hamburg, Germany and University of Hamburg, Germany  
 † and Czech Technical University, Prague, Czech Republic

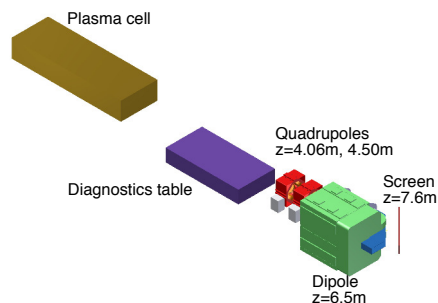


Figure 1: A 3D CAD image of the spectrometer system annotated with distances along the  $z$  direction from the exit of the plasma cell to the magnetic centres of magnets, and the centre of the scintillator screen.

Resolution below). It was finally decided to change the design and to use magnet HB4 instead of MBPS since HB4 has sufficient field strength and field width (see Table 1), and similar resolution to MBPS.

Table 1: Comparison Between Window-shaped Dipole MBPS and C-shaped Dipole HB4 [7].

Dipole	MBPS	HB4
<b>Weight</b>	15 t	8.5 t
<b>Power consumption</b>	60 kW	24 kW cycled
<b>Integrated field</b>	1.9 Tm	1.6 T cycled
<b>Max. mag. field</b>	1.65 T	1.5 T cycled
<b>Hor. aper.</b>	52 cm	32 cm
<b>Vert. aper.</b>	11 cm	8 cm
<b>Iron length</b>	1 m	1 m

**Field maps and measurements** Field measurements have been carried out [7] on the HB4 field at the magnetic centre and the integrated field has been measured along a line parallel to the  $z$ -axis running through the magnetic centre. Three dimensional field maps [8] calculated using the OPERA simulation software at various field strengths show agreement with the measurements to within 2-3% (Table 2), with fields calculated for 100 A, 170 A, 540 A and 650 A.

The measurable energy range can be set by changing the magnet current. The simulation results giving the currents and corresponding ranges are shown in Table 3. The magnet current can, of course, be set to intermediate values.

Table 2: Magnetic Field Measurements (and OPERA Simulation Results).  $B_y$  is measured at the magnetic centre, (0,0,0), and  $\int B_y$  is calculated along the z-axis.

$I$ [A] (sim.)	$B_y$ [T]	$\int B_y$ [T] (sim.)
0	$2 \times 10^{-4}$	$2.3 \times 10^{-4}$
39.98 (40)	0.1276 (0.1265)	0.1433 (0.1422)
240.26 (240)	0.7651 (0.715)	0.8563 (0.8510)
320.07 (320)	1.0135 (1.0043)	1.1257(1.1116)
400.13 (400)	1.2193 (1.1937)	1.3355 (1.3056)

Table 3: The approximate highest and lowest measurable energy for each available field map for the reference electron trajectory. Also shown is the energy of electrons hitting the centre of the screen.

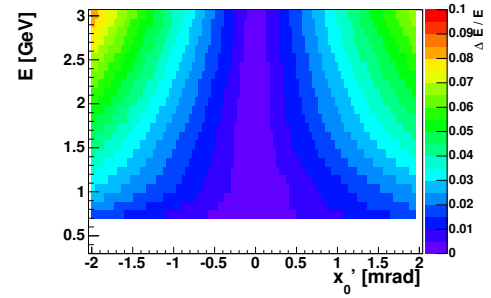
$I$ [A]	$E_{\text{low}}$ [MeV]	$E_{\text{centre}}$ [MeV]	$E_{\text{high}}$ [GeV]
0	0.521	0.555	0.003
40	56	145	1.966
100	140	363	4.38
170	238	618	8.317
240	335	869	11.77
320	438	1133	15.35
400	516	1327	17.93
540	580	1487	19.94
650	609	1599	20.81

### Resolution

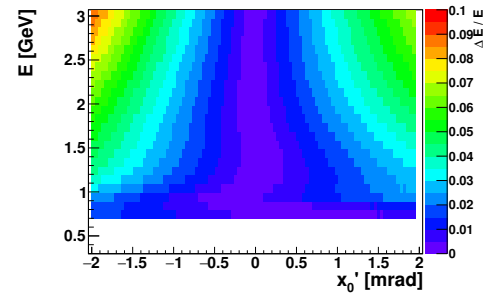
Any deviation of a particle from the reference trajectory will cause a shift in the measured energy,  $\Delta E$ . The initial electron beam position, horizontal angular spread and mean angular trajectory of the beam are unknown but are limited by the transverse size of the accelerating plasma column. The maximum position and angular offsets of the beam are estimated to be 1 mm and  $\sim 2$  mrad at the exit of the plasma cell. The angular offset dominates because this transforms to a position offset at the screen of  $\sim 16$  mm.

To compare the resolutions of MBPS and HB4, the field map for MBPS was scaled so that the two field maps had the same  $\int B dz$ . A model of the spectrometer was built using BDSIM [9], a beam line simulation toolkit including particle-matter interactions based on GEANT4 [10]. The field maps were loaded into the BDSIM model (with the quadrupoles turned off) of the spectrometer system geometry and  $\Delta E/E$  was plotted for a range of energies and angles (Figure 2). In the energy and angle ranges plotted the HB4 uncertainty is not significantly worse than that of MBPS.

To calculate the maximum energy uncertainty, a "positive" beam is defined, which is a pencil beam offset in angle by 2 mrad and in position by 1 mm in the positive  $x$  direction (towards the screen) and a "negative" beam at  $-2$  mrad and  $-1$  mm, giving the maximum positive and negative deviations of the energy measurements from the true energy. These are plotted as a function of energy for a range of field maps (with the quadrupoles turned off) in Fig. 3. This shows



(a) Window-shaped dipole MBPS. Field map is scaled so that  $\int B dz$  is the same as that of HB4 at  $B=1.43$ T (Fig. 2b)



(b) C-shaped dipole HB4.  $B=1.43$  T

Figure 2: Uncertainty of energy measurement as a function of energy and angle.

the importance of setting the correct dipole current to obtain the best resolution for a given energy range.

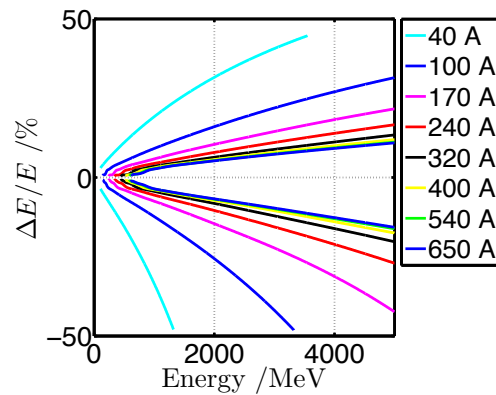


Figure 3:  $\Delta E/E$  vs. energy for dipole HB4 at various magnet current settings.

### Quadrupole Focusing

A quadrupole doublet is placed upstream of the dipole as shown in Fig. 1. The doublet will focus the electron beam both vertically and horizontally as shown in Fig. 4. The benefits are therefore twofold: to reduce the energy measurement uncertainty directly, and through increasing the signal to background ratio of the system by increasing

the electron density at the screen and therefore light yield per pixel at the CCD camera.

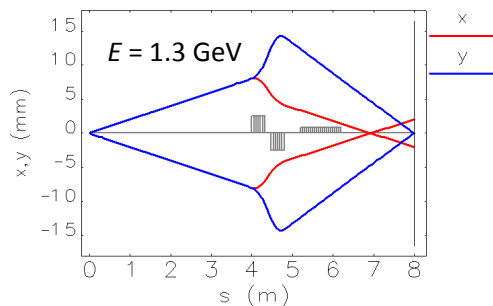


Figure 4: ELEGANT [11] simulation results showing the trajectories of electrons with angles at the plasma cell of  $\pm 2$  mrad. The first quadrupole has  $K_1 = +4.07 \text{ m}^{-2}$  and the second quadrupole has  $K_1 = -4.07 \text{ m}^{-2}$ .

For a given quadrupole gradient,  $\Delta E/E$  will be minimised for a different energy. Energies greater or lesser than this will be over- or under-focused. Given that the witness beam will have an unknown energy spread, care must be taken with the initial quadrupole settings. The quadrupoles currently proposed have a maximum field strength of 18.1 T/m, which will optimally focus a beam at  $\sim 1.3$  GeV. Initially, the dipole is likely to be set to somewhere between 0 and 40 A in order to be able to view low energy electrons. A 40 A field map (simulated) was used in the BDSIM simulation and  $\Delta E/E$  was plotted as a function of energy and quadrupole field strengths. The plot for the "negative" beam is shown in Fig. 5. This shows that the energy resolution can be greatly improved in the few hundred MeV range of energies around the peak energy, however, low energy beams can be over focused and lost. Plots such as these have been produced for the full range of HB4 field maps.

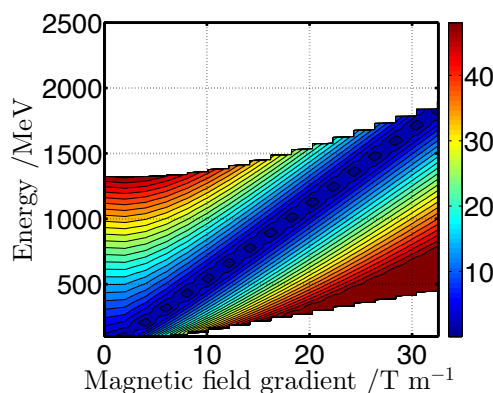


Figure 5:  $\Delta E/E$  as a function of energy and quadrupole strength with the HB4 dipole current at 40A for the "negative" beam.

### SIGNAL TO BACKGROUND RATIO

A FLUKA [12] simulation was carried out to calculate the backgrounds reaching the downstream end of the plasma

cell. 15 million protons from the SPS were tracked along the AWAKE beam line [13]. A 0.2 mm thick aluminium window included in the simulation will be required in order to protect the vacuum in the SPS. The resulting particles, distributed across the whole of the tunnel at the exit of the plasma cell, were then tracked from the end of the plasma cell through the BDSIM spectrometer simulation. The resulting optical photons emitted from the spectrometer's scintillator screen were recorded. The distributed optical photon emissions due to these backgrounds were then compared to the expected optical photon distribution due to the witness electron beam signal in order to calculate the signal to background ratio (Fig. 6), showing a peak signal to background ratio of  $\sim 1000$ .

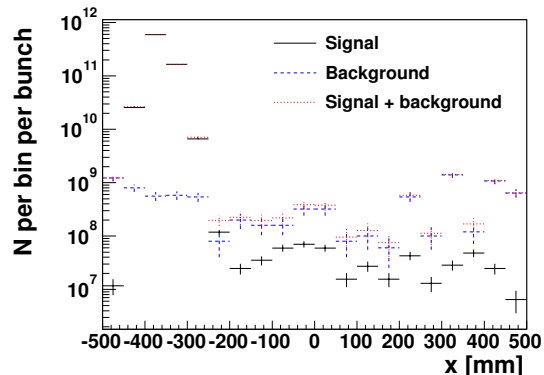


Figure 6: Optical photons emitted from the screen due to signal (witness electrons) and background in the screen with the 0.2 mm thick aluminium window separating the AWAKE beam line from the SPS.

### CONCLUSIONS

Studies have been carried out regarding energy measurement uncertainties for a range of spectrometer settings and an alternative dipole magnet. The energy uncertainty can be greatly improved with appropriate settings depending on the energy profile of the witness electron beam. The HB4 dipole was selected to replace MBPS. A peak signal to background ratio in terms of flux density of optical photons emitted from the screen was calculated as  $\sim 1000$ , given a 0.2 mm aluminium vacuum window separating the AWAKE beam line from the SPS. Due to the radiation environment in the AWAKE experimental area, the CCD camera will have to be moved  $\sim 20$  m away to the adjacent tunnel. Work is ongoing to design an optical line to transport the light from the screen to the camera.

### ACKNOWLEDGMENT

M. Wing acknowledges the support of DESY, Hamburg, and the Alexander von Humboldt Foundation. The work is part of EuCARD-2, partly funded by the European Commission, GA 312453.

## REFERENCES

- [1] R. Assman *et al.*, “Proton drive plasma wakefield acceleration: a path to the future of high-energy physics”, *Plasma Phys. Control. Fusion* **56** 084013 (2013)  
<http://iopscience.iop.org/0741-3335/56/8/084013>
- [2] A. Caldwell *et al.*, “AWAKE Design Report: A Proton-Driven Plasma Wakefield Acceleration Experiment at CERN”, CERN-SPSC-2013-013 (2013)  
<http://cds.cern.ch/record/1537318>
- [3] E. Gschwendtner *et al.*, “Performance and Operational Experience of the CNGS Facility”, IPAC’10, THPEC046, p. 4164–4166 (2010),  
<http://jacow.org/IPAC10/papers/thpec046.pdf>
- [4] K. Lotov *et al.*, “Natural noise and external wakefield seeding in a proton-driven plasma accelerator”, *Phys. Rev. ST Accel. Beams* **16** (4), 041301 (2013),  
<http://link.aps.org/doi/10.1103/PhysRevSTAB.16.041301>
- [5] S. Jolly, L. Deacon, J. Goodhand, S. Mandry, and M. Wing, “A Spectrometer for Proton Driven Plasma Wakefield Accelerated Electrons at AWAKE”, IPAC’14, TUPME079, p. 1540–1543(2014),  
<http://accelconf.web.cern.ch/AccelConf/IPAC2014/papers/tupme079.pdf>
- [6] E. Gschwendtner *et al.*, “The AWAKE Experimental Facility at CERN”, IPAC’14, MOPRI005, p. 582–585 (2014),  
<http://accelconf.web.cern.ch/AccelConf/IPAC2014/papers/mopri005.pdf>
- [7] “Specification of the Bending Magnets for the ISR Beam Transfer System”, CERN, I-5010-ISR, 7th November 1967,  
<https://edms.cern.ch/file/1100428/1/1100428.pdf>
- [8] A. Vorozhtsov, *private communication*, CERN.
- [9] S. T. Boogert *et al.*, “Beam Delivery Simulation (BDSIM): A Geant4 Based Toolkit for Diagnostic and Loss Simulation”, IBIC’13, WEPC46, p. 799–802 (2013),  
<http://jacow.org/IBIC2013/papers/wepc46.pdf>
- [10] S. Agostinelli *et al.*, “Geant4 — a simulation toolkit”, *Nucl. Instr. Meth. A*, **506** (3), p.250–303 (2003),  
[http://dx.doi.org/10.1016/S0168-9002\(03\)01368-8](http://dx.doi.org/10.1016/S0168-9002(03)01368-8)
- [11] “Features and Applications of the Program Elegant”, IPAC’13, THPPA02, p. 3139-3142 (2013),  
<http://accelconf.web.cern.ch/AccelConf/IPAC2013/papers/thppa02.pdf>
- [12] G. Battistoni, S. Muraro, P. R. Sala, F. Cerutti, A. Ferrari, S. Roesler, A. Fasso and J. Ranft, “The FLUKA code: Description and benchmarking,” *AIP Conf. Proc.* **896** (2007) 31.
- [13] P. Ortega, *private communication*, CERN.